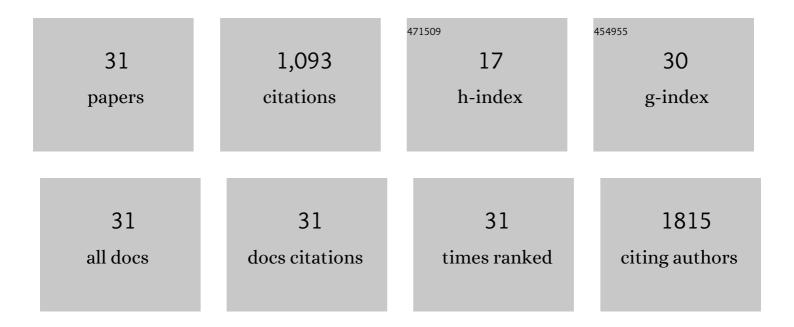
Wang-Chang Geng

List of Publications by Year in descending order

Source: https://exaly.com/author-pdf/7530798/publications.pdf Version: 2024-02-01



#	Article	IF	CITATIONS
1	Effect of large pore size of multifunctional mesoporous microsphere on removal of heavy metal ions. Journal of Hazardous Materials, 2013, 254-255, 157-165.	12.4	128
2	Ordered Mesoporous Copper Oxide with Crystalline Walls. Angewandte Chemie - International Edition, 2007, 46, 738-741.	13.8	124
3	Thermal percolation behavior of graphene nanoplatelets/polyphenylene sulfide thermal conductivity composites. Polymer Composites, 2014, 35, 1087-1092.	4.6	113
4	Thermal conductivities, mechanical and thermal properties of graphite nanoplatelets/polyphenylene sulfide composites. RSC Advances, 2014, 4, 22101-22105.	3.6	98
5	Volatile Organic Compound Gas-Sensing Properties of Bimodal Porous α-Fe ₂ O ₃ with Ultrahigh Sensitivity and Fast Response. ACS Applied Materials & Interfaces, 2018, 10, 13702-13711.	8.0	87
6	Hollow Mesoporous SiO ₂ –BiOBr Nanophotocatalyst: Synthesis, Characterization and Application in Photodegradation of Organic Dyes under Visible-Light Irradiation. ACS Sustainable Chemistry and Engineering, 2015, 3, 1101-1110.	6.7	54
7	A novel highly crystalline Fe ₄ (Fe(CN) ₆) ₃ concave cube anode material for Li-ion batteries with high capacity and long life. Journal of Materials Chemistry A, 2019, 7, 11478-11486.	10.3	50
8	Ordered Large-Pore Mesoporous Cr ₂ O ₃ with Ultrathin Framework for Formaldehyde Sensing. ACS Applied Materials & Interfaces, 2017, 9, 18170-18177.	8.0	47
9	Morphology-Dependent Gas Sensing Properties of CuO Microstructures Self-Assembled from Nanorods. Sensors and Actuators B: Chemical, 2020, 325, 128775.	7.8	42
10	Effect of framework structure, pore size and surface modification on the adsorption performance of methylene blue and Cu2+ in mesoporous silica. Colloids and Surfaces A: Physicochemical and Engineering Aspects, 2018, 539, 154-162.	4.7	39
11	Remarkable humidity-responsive sensor based on poly (N,N-diethylaminoethyl) Tj ETQq1 1 0.784314 rgBT /Ove	rlock 10 Tf	50,342 Td (n
12	Pore size dependent acetic acid gas sensing performance of mesoporous CuO. Sensors and Actuators B: Chemical, 2021, 334, 129639.	7.8	31
13	Surface modification of HMPBO fibers by silane coupling agent of KH-560 treatment assisted by ultrasonic vibration. Fibers and Polymers, 2012, 13, 979-984.	2.1	30
14	Ultrahigh humidity sensitivity of NaCl-added 3D mesoporous silica KIT-6 and its sensing mechanism. RSC Advances, 2016, 6, 38391-38398.	3.6	27
15	The self-assembly of octahedral CuxO and its triethylamine-sensing properties. Sensors and Actuators B: Chemical, 2020, 312, 128014.	7.8	23
16	Synthesis of rattle-type magnetic mesoporous Fe ₃ O ₄ @mSiO ₂ @BiOBr hierarchical photocatalyst and investigation of its photoactivity in the degradation of methylene blue. RSC Advances, 2015, 5, 48050-48059.	3.6	20
17	Humidity sensing performance of mesoporous CoO(OH) synthesized via one-pot hydrothermal method. Sensors and Actuators B: Chemical, 2019, 280, 46-53.	7.8	18
18	Synthesis of hollow spherical nickel oxide and its gas-sensing properties. Rare Metals, 2021, 40, 1622-1631.	7.1	16

WANG-CHANG GENG

#	Article	IF	CITATIONS
19	Preparation of nanoparticles and hollow spheres of α-Fe2O3 and their properties. Research on Chemical Intermediates, 2011, 37, 389-395.	2.7	15
20	Fabrication of 1D Fe3O4/P(NIPAM-MBA) thermosensitive nanochains by magnetic-field-induced precipitation polymerization. Colloid and Polymer Science, 2012, 290, 1207-1213.	2.1	15
21	Efficient Photocatalytic Degradation of Dyes over Hierarchical BiOBr/βâ€Co(OH) ₂ /PVP Multicomponent Photocatalyst under Visibleâ€Light Irradiation. ChemCatChem, 2015, 7, 4163-4172.	3.7	15
22	Removal of Cationic Dyes, Heavy Metal Ions, and CO2 Capture by Adsorption on Mesoporous Silica HMS. Water, Air, and Soil Pollution, 2017, 228, 1.	2.4	14
23	Humidity Sensing Property of NaClâ€Added Mesoporous Silica Synthesized by a Facile Way with Low Energy Cost. International Journal of Applied Ceramic Technology, 2015, 12, 169-175.	2.1	11
24	Fabrication and characterization of 1 D Fe3O4/P(NIPAM–MAA–MBA) nanochains with thermo- and pH-responsive shell for controlled release for phenolphthalein. Journal of Materials Science, 2015, 50, 3083-3090.	3.7	10
25	Effect of Sb doping on structural and photoelectric properties of SnO2 thin films. Journal of Materials Science: Materials in Electronics, 2020, 31, 3289-3302.	2.2	10
26	Preparation of monodispersed α-Fe2O3 nanoparticles by a hydrothermal synthetic route. Research on Chemical Intermediates, 2011, 37, 523-529.	2.7	8
27	Preparation and characterization of structure-tailored magnetic fluorescent Fe3O4/P(GMA–EGDMA–NVCz) core–shell microspheres. Journal of Materials Science, 2013, 48, 5302-5308.	3.7	7
28	Transparent and conducting Ga-doped ZnO films on flexible substrates prepared by sol–gel method. Journal of Materials Science: Materials in Electronics, 2017, 28, 8669-8674.	2.2	5
29	Investigation of selective etching mechanism and its dependency on the particle size in preparation of hollow silica spheres. Journal of Nanoparticle Research, 2015, 17, 1.	1.9	2
30	Preparation of High Value Added Activated Carbons from Corncob for Electric Double Layer Capacitors. Journal of Nanoscience and Nanotechnology, 2017, 17, 3803-3808.	0.9	2
31	Mediated electrochemistry of dimethyl sulfoxide reductase promoted by carbon nanotubes. Science China Chemistry, 2010, 53, 2560-2563.	8.2	0